Stem Cell Reports
Article

ISSCR

OPEN ACCESS

Retinal Ganglion Cells With a Glaucoma OPTN(E50K) Mutation Exhibit Neurodegenerative Phenotypes when Derived from Three-Dimensional Retinal Organoids

Kirstin B. VanderWall,[1,7] Kang-Chieh Huang,[1,7] Yanling Pan,[2] Sailee S. Lavekar,[1] Clarisse M. Fligor,[1] Anna R. Allsop,[1] Kelly A. Lentsch,[1] Pengtao Dang,[3] Chi Zhang,[3] Henry C. Tseng,[4] Theodore R. Cummins,[1,5] and Jason S. Meyer[1,3,5,6,*]

[1]Department of Biology, Indiana University Purdue University Indianapolis, Indianapolis, IN 46202, USA
[2]Indiana BioMedical Gateway Program, Indiana University School of Medicine, Indianapolis, IN 46202, USA
[3]Department of Medical and Molecular Genetics, Indiana University School of Medicine, Indianapolis, IN 46202, USA
[4]Duke Eye Center and Department of Ophthalmology, Duke University Medical Center, Durham, NC 27710, USA
[5]Stark Neurosciences Research Institute, Indiana University School of Medicine, Indianapolis, IN 46202, USA
[6]Department of Ophthalmology, Glick Eye Institute, Indiana University School of Medicine, Indianapolis, IN 46202, USA
[7]Co-first author
*Correspondence: meyerjas@iu.edu
https://doi.org/10.1016/j.stemcr.2020.05.009

SUMMARY

Retinal ganglion cells (RGCs) serve as the connection between the eye and the brain, with this connection disrupted in glaucoma. Numerous cellular mechanisms have been associated with glaucomatous neurodegeneration, and useful cellular models of glaucoma allow for the precise analysis of degenerative phenotypes. Human pluripotent stem cells (hPSCs) serve as powerful tools for studying human disease, particularly cellular mechanisms underlying neurodegeneration. Thus, efforts focused upon hPSCs with an E50K mutation in the Optineurin (OPTN) gene, a leading cause of inherited forms of glaucoma. CRISPR/Cas9 gene editing introduced the OPTN(E50K) mutation into existing lines of hPSCs, as well as generating isogenic controls from patient-derived lines. RGCs differentiated from OPTN(E50K) hPSCs exhibited numerous neurodegenerative deficits, including neurite retraction, autophagy dysfunction, apoptosis, and increased excitability. These results demonstrate the utility of OPTN(E50K) RGCs as an *in vitro* model of neurodegeneration, with the opportunity to develop novel therapeutic approaches for glaucoma.

INTRODUCTION

Glaucoma is a devastating optic neuropathy which causes the progressive degeneration of retinal ganglion cells (RGCs), leading to irreversible loss of vision and eventual blindness (Gupta and Yucel, 2007; Hartwick, 2001; Quigley, 2011). Various animal models have been developed that have led to a greater understanding of glaucomatous neurodegeneration (Agostinone and Di Polo, 2015; Cueva Vargas et al., 2015; Kalesnykas et al., 2012; Williams et al., 2013), although these models often exhibit physiological features that do not precisely reflect those present within human patients. Furthermore, recent studies demonstrating significant variability between rodent and primate RGCs (Peng et al., 2019) suggest that there may be important differences in how these cells respond to glaucomatous injuries between species. As such, there is a strong need to develop new approaches to complement these glaucoma models to determine RGC pathogenesis and mechanisms leading to their degeneration and death.

Human pluripotent stem cells (hPSCs) provide an attractive option as a model for studies of cellular development and disease progression as they can be cultured indefinitely and induced to differentiate into all cell types of the body (Thomson et al., 1998), including RGCs (Fligor et al., 2018; Langer et al., 2018; Ohlemacher et al., 2016; Sluch et al., 2017; Tanaka et al., 2015; Teotia et al., 2017a; VanderWall et al., 2019). When harboring genetic mutations associated with disease states, the derivation of these cells from patient-specific sources allows for the ability to study mechanisms underlying diseases, such as glaucoma (Inagaki et al., 2018; Minegishi et al., 2013; Ohlemacher et al., 2016; Teotia et al., 2017b). In addition, gene-editing approaches, including CRISPR/Cas9 technology allow for the ability to create isogenic controls from these patient-derived cells and also introduce disease-causing mutations in unaffected cells, leading to the generation of new disease models (Cong et al., 2013; Muffat et al., 2016; Poon et al., 2017). Among the gene mutations associated with glaucoma, those mutations in the Optineurin (OPTN) gene are known to result in glaucomatous neurodegeneration in the absence of increased intraocular pressure (Fingert, 2011; Minegishi et al., 2016; Sarfarazi et al., 2003). These mutations directly affect RGCs, with the OPTN(E50K) mutation previously shown to result in a particularly severe degenerative phenotype (Chalasani et al., 2014; Inagaki et al., 2018; Meng et al., 2012; Rezaie et al., 2002; Tseng et al., 2015; Ying et al., 2015). As such, the generation of hPSCs harboring the OPTN(E50K) mutation, along with corresponding isogenic controls, allows for the *in vitro*

analysis of mechanisms underlying the degeneration of RGCs in glaucoma.

Thus, the efforts of the current study were initially focused upon the generation of hPSCs with the OPTN(E50K) mutation as well as their corresponding isogenic controls through the use of CRISPR/Cas9 gene editing. Upon initial differentiation of these cells into three-dimensional retinal organoids and subsequent RGC purification, OPTN(E50K) and isogenic control cells both developed in a similar manner, yielding a comparable number of RGCs. Conversely, at later stages of RGC maturation, OPTN(E50K) RGCs demonstrated numerous characteristics associated with glaucomatous neurodegeneration, including neurite retraction, autophagy dysfunction, and increased excitability. The results of this study provide the most comprehensive analysis of glaucomatous neurodegeneration to date using hPSC-based models, including the demonstration of CRISPR/Cas9 gene editing to provide essential disease models and corresponding isogenic controls for glaucoma.

RESULTS

CRISPR/Cas9-Edited OPTN(E50K) Disease Models and Isogenic Controls

The ability to precisely edit genes in hPSCs through CRISPR/Cas9 gene-editing technology allows for new insights into disease modeling, including the generation of isogenic controls (Cong et al., 2013; Muffat et al., 2016; Poon et al., 2017). When properly applied, CRISPR/Cas9 gene editing allows for the enhanced ability to analyze disease phenotypes due to relevant mutations by minimizing genetic variability between cell lines. As such, CRISPR/Cas9 gene editing was utilized in the current study to examine the E50K mutation in the OPTN protein, a known genetic determinant for glaucoma.

To introduce the OPTN(E50K) mutation in hPSCs (Figure 1), the homology-directed repair (HDR) template was designed to include the mutant nucleotide c.458G > A that altered the 50th amino acid from glutamic acid (E) to lysine (K), with an additional two silent mutations (c.454G > C and c.460G > A). The first silent mutation altered an Hpy188III restriction site, which was used for PCR screening of prospective gene-edited clones. The second silent mutation was introduced to prevent Cas9 from cutting the donor template by modifying the PAM site. A plasmid containing the OPTN(E50K) HDR template as well as the guide RNA was co-transfected with pCas9-GFP, with the GFP signal used to sort for presumptively edited cells (Figures 1A–1C). Clonal populations were screened by PCR amplification of the edited region and enzymatic digestion with Hpy188III, with prospectively edited clones further sequenced to ensure proper editing of the target gene (Figure 1D). Likewise, patient-specific hiPSCs harboring the OPTN(E50K) mutation utilized a similar strategy to correct the OPTN(E50K) mutation (Figure 1E). Following CRISPR/Cas9 gene editing, the karyotypes of each cell line were analyzed to reveal normal karyotypes (Figure S1). The results of these experiments demonstrated the successful establishment of hPSC lines harboring the OPTN(E50K) mutation along with their corresponding isogenic controls.

OPTN(E50K) Glaucomatous RGCs Demonstrate Morphological Deficits and Gene Downregulation after Prolonged Culture

The degeneration of RGCs in glaucoma severely affects the visual pathway, leading to blindness (Fingert, 2011; Gupta and Yucel, 2007; Hartwick, 2001; Quigley, 2011). This degeneration is commonly associated with advanced age, as the initial development of the retina is unaffected by the disease state. As such, the early differentiation of OPTN(E50K) and isogenic control hPSCs yielded similar formation of optic vesicle-like and optic cup retinal organoids and a comparable number of RGCs (Figure 2).

Previous studies in animal models of RGC damage have demonstrated significant neurite retraction and dendritic remodeling in response to RGC injury and disease (Agostinone and Di Polo, 2015; Agostinone et al., 2018; Kalesnykas et al., 2012; Williams et al., 2013). To examine if this phenomenon could be recapitulated in an hPSC model, OPTN(E50K) and isogenic control RGCs were examined in a temporal fashion for morphological characteristics associated with neuronal maturation (Figure 3). Representative inverted fluorescent images (Figures 3A–3H) and neurite tracings (Figures 3I–3P) of OPTN(E50K) and isogenic control RGCs revealed high degrees of similarity in neuronal maturation from 1 to 3 weeks after purification. By 4 weeks of maturation, however, OPTN(E50K) RGCs displayed deficits in neurite complexity, cell body size, and neurite length (Figures 3Q–3S), as well as in the expression of various synaptic proteins (Figure S2). These results suggested that OPTN(E50K) and isogenic control RGCs exhibited similar morphological profiles during the early stages but, following maturation, OPTN(E50K) RGCs significantly reduced their morphological complexity, similar to what has been previously observed for glaucomatous RGCs *in vivo*.

Previous studies in animal models of RGC injury have also demonstrated the downregulation of RGC-associated proteins before the degeneration of these cells (Soto et al., 2008; Weishaupt et al., 2005). As such, efforts were made to determine if RGC-associated proteins were similarly downregulated in OPTN(E50K) RGCs (Figure 4). As a percentage of the total cell population, the

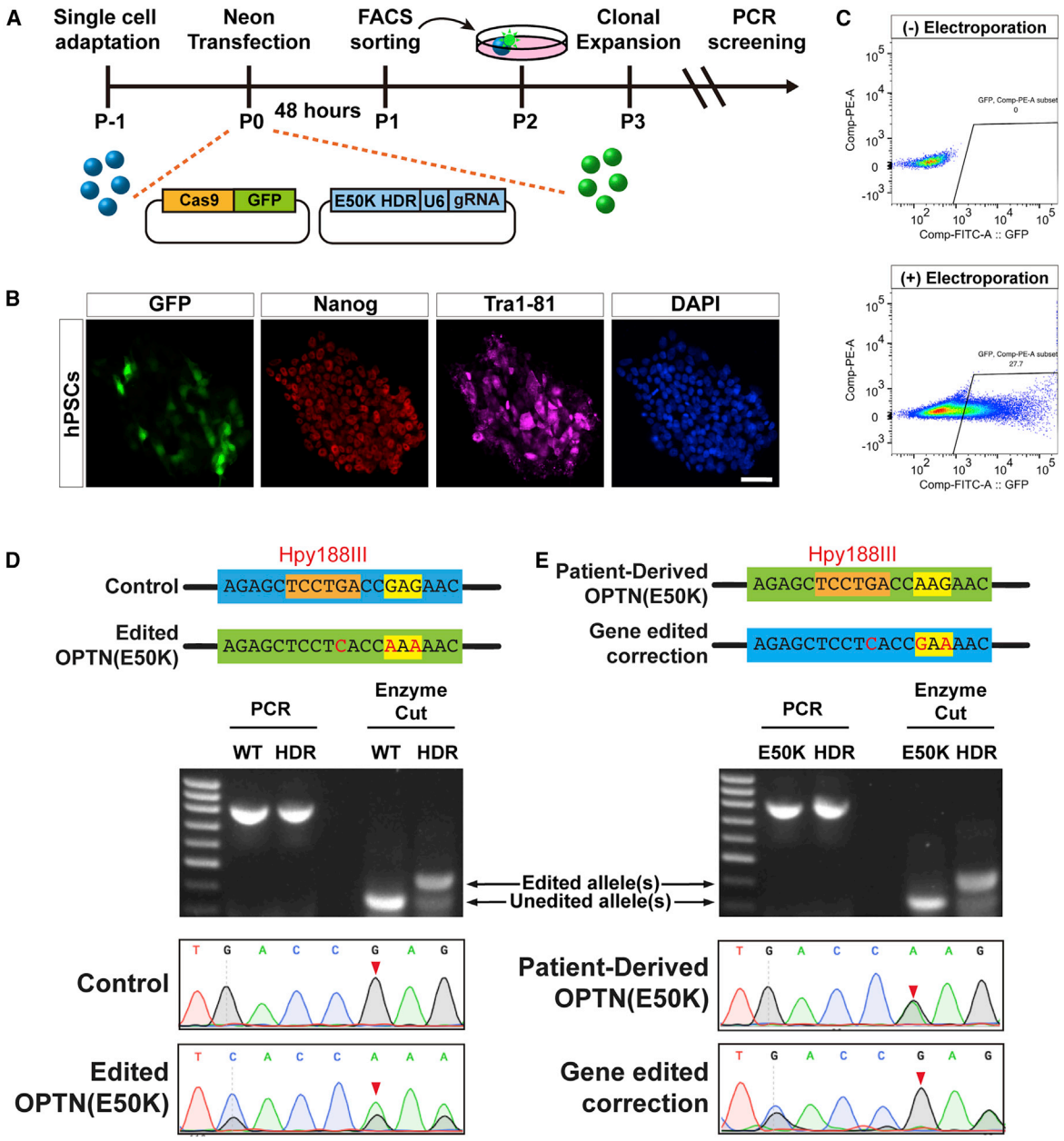

Figure 1. CRISPR/Cas9 Gene Editing for the Generation of OPTN(E50K) hPSCs and Corresponding Isogenic Controls

(A) Schematic displaying the workflow for the CRISPR/Cas9 gene editing of hPSCs.

(B) A subset of GFP-positive cells was observed in hPSCs expressing Nanog and Tra1-81 after electroporation.

(C) Flow cytometry indicated the gating of GFP-positive cells 48 h after electroporation.

(D and E) CRISPR/Cas9-edited cells were screened for the insertion of the OPTN(E50K) mutation in wild-type hPSCs (D) and correction of the mutation in patient-derived hPSCs (E) by restriction digestion with Hpy188III and Sanger sequencing. The 50th codon of the OPTN gene is highlighted in yellow. The red arrows highlight the insertion or correction of the OPTN(E50K) missense mutation site in Sanger sequencing. Scale bar, 50 μm (B).

expression of the RGC transcription factors BRN3B and ISL1 were significantly decreased in OPTN(E50K) RGCs compared with isogenic controls (Figures 4A and 4B). To determine if this decrease was a result of gene down-regulation or loss of cells, the expression of each was compared with the expression of the RGC-associated cytoskeletal marker MAP2. No significant differences were observed in the percentage of MAP2-positive cells

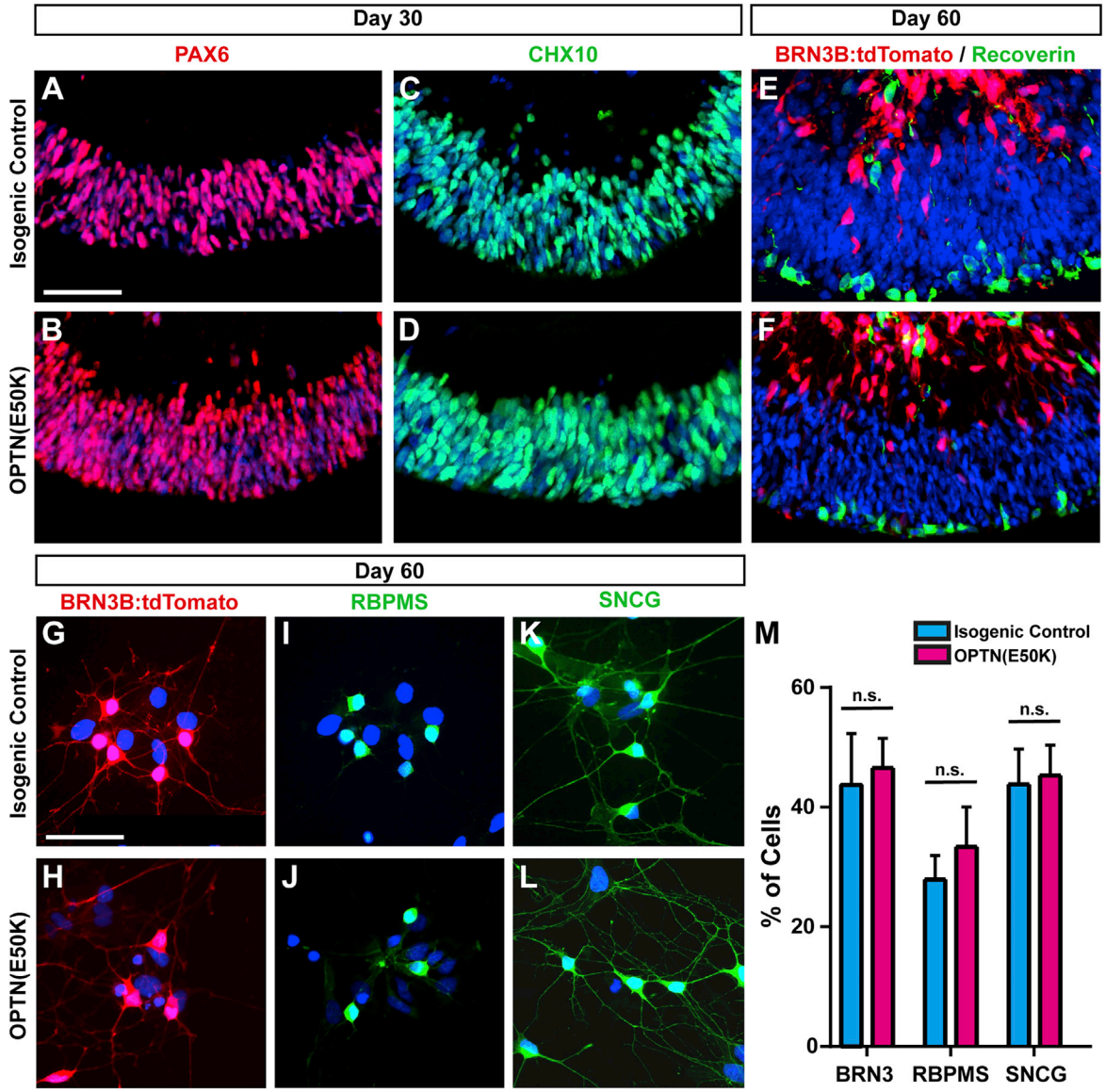

Figure 2. The OPTN(E50K) Mutation Does Not Affect Early Stages of Retinal Differentiation

(A–D) Immunocytochemistry analyzed the expression of PAX6 (A and B) and CHX10 (C and D) at 30 days of differentiation, revealing no significant differences between OPTN(E50K) and isogenic control retinal organoids.

(E and F) Similarly, both conditions demonstrated similar expression patterns for BRN3B:tdTomato within inner layers and Recoverin within outer layers of retinal organoids after 60 days of differentiation.

(G–M) RGCs dissociated from OPTN(E50K) (H, J, and L) and isogenic control (G, I, and K) retinal organoids demonstrated no significant differences in the expression of BRN3B:tdTomato, RBPMS, and SNCG (M). Error bars represent SEM (n = 5 separate differentiation experiments each using OPTN(E50K) hiPSCs, OPTN- corrected hiPSCs, and H7 and H7(E50K) hPSCs). Scale bars, 100 μm (A–F) and 50 μm (G–L).

between OPTN(E50K) and isogenic control RGCs; however, the colocalization of either BRN3B or ISL1 with MAP2 was significantly reduced in the OPTN(E50K) condition. Conversely, retinal progenitor cells and photoreceptors were unaffected by the OPTN(E50K) mutation, with a specific loss of BRN3-expressing RGCs (Figures 4C and 4D). Minimal colocalization was identified between MAP2 and retinal progenitors or photoreceptors marked by CHX10, recoverin, and OTX2, suggesting a high specificity of MAP2 to RGCs (Figures 4E–4G). These results suggested an early downregulation of RGC-associated transcription factors in response to the OPTN(E50K)

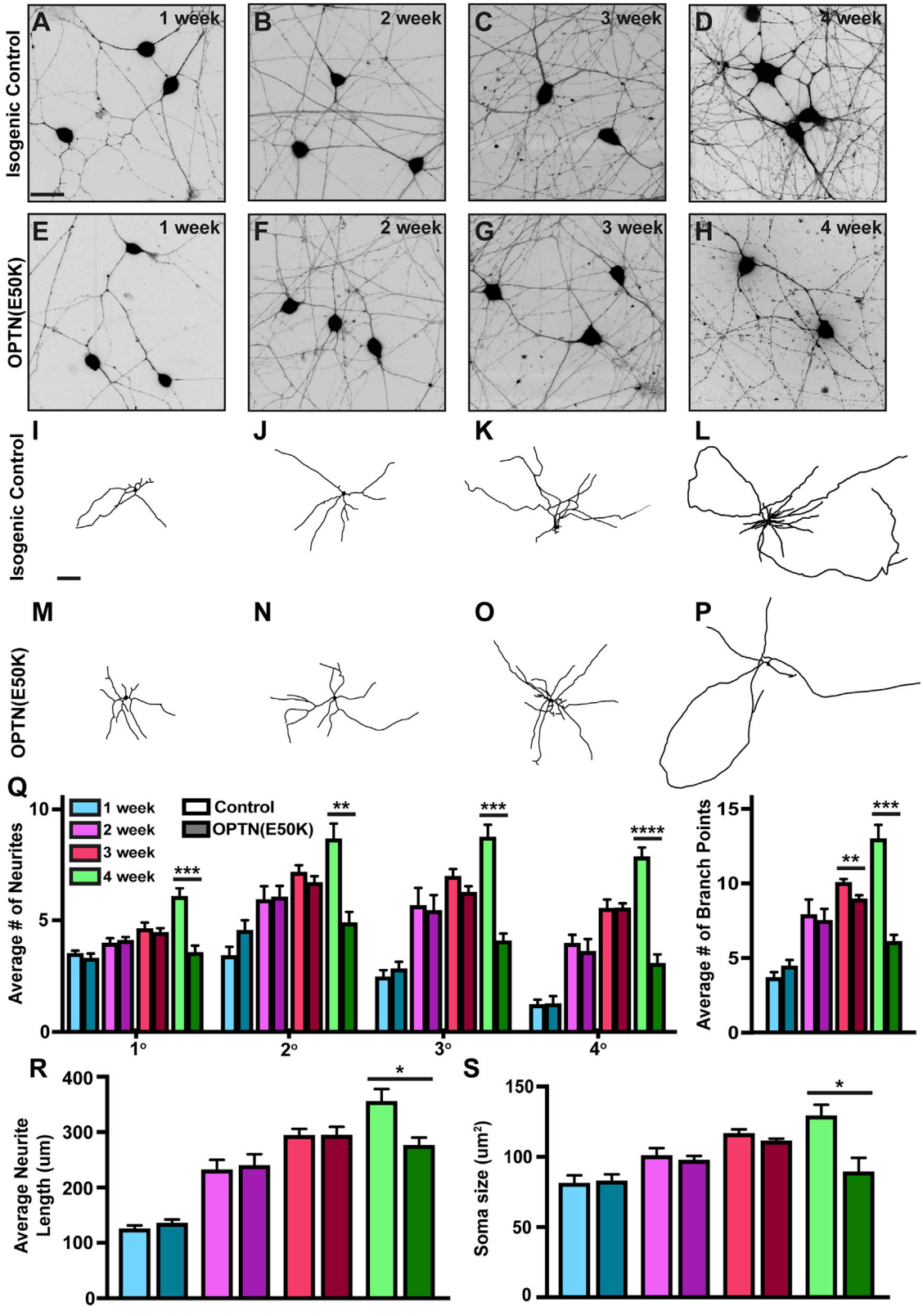

(legend on next page)

mutation, indicative of an increased susceptibility to subsequent glaucomatous neurodegeneration.

Functional Consequences of the OPTN(E50K) Glaucomatous Mutation

Previous studies have demonstrated changes in RGC excitability associated with the glaucomatous disease state (Cueva Vargas et al., 2015) and, as such, patch-clamp analyses determined if functional changes were present in OPTN(E50K) RGCs (Figure 5). Within 4 weeks of RGC maturation, both OPTN(E50K) and isogenic control RGCs demonstrated functional properties, including ionic currents as well as spontaneous firing of action potentials (Figures 5A and 5B). No significant changes were detected in the resting membrane potential (Figure 5C), although OPTN(E50K) RGCs displayed a significantly lower cell capacitance, higher input resistance, as well as lower action potential current threshold (Figures 5D–5F), suggesting possible changes to excitable properties. To test this, current-clamp recordings demonstrated that OPTN(E50K) RGCs fired significantly more action potentials (Figures 5G and 5H). These results demonstrated an increased excitability of OPTN(E50K) RGCs, suggesting that excitotoxicity may play a key role in the early stages of RGC degeneration in glaucoma.

RNA Sequencing Demonstrated Differential Gene Expression in OPTN(E50K) RGCs

To elucidate gene expression differences and the specific cellular pathways affected by the OPTN(E50K) mutation, RNA sequencing was conducted on RGCs purified from OPTN(E50K) and isogenic control retinal organoids (Figure 6). Initial analysis demonstrated 75 downregulated genes and 117 upregulated genes associated with OPTN(E50K) RGCs when compared with isogenic control RGCs (Figure 6B). Of the downregulated genes, a number of genes were associated with the clearance of aggregated proteins, protein trafficking, and neurite outgrowth. Pathway analyses revealed changes in gene expression associated with a variety of neurodegenerative diseases, including amyotrophic lateral sclerosis (ALS) and Alzheimer disease, as well as the downregulation of pathways related to autophagy and neurite outgrowth (Figure 6C). Thus, as RNA sequencing results demonstrated differential gene expression and pathways suggesting autophagy dysfunction, opportunities to examine deficits in autophagy associated with this mutation were further pursued.

OPTN(E50K) RGCs Exhibit Autophagy Disruption and Increased Susceptibility to Apoptosis

The OPTN protein plays an important role as an autophagy receptor (Minegishi et al., 2016; Sirohi and Swarup, 2016; Slowicka et al., 2016; Ying and Yue, 2016), with mutations to the OPTN protein, such as the E50K mutation disrupting the autophagy pathway leading to the damage and degeneration of RGCs (Chalasani et al., 2014; Inagaki et al., 2018; Meng et al., 2012; Minegishi et al., 2013; Ying et al., 2015). As such, to elucidate possible disruptions to the autophagy pathway, retinal organoids were examined for the expression of LC3, particularly the accumulation of this protein as a hallmark of autophagy dysfunction (Figure 7). Compared with isogenic controls, OPTN(E50K) organoids exhibited profound LC3 accumulation exclusively within inner layers where RGCs reside, indicating a differential effect upon these cells (Figures 7A–7F). To test the possibility of rescuing this phenotype, the autophagy pathway was enhanced through treatment with rapamycin, leading to a significant reduction of LC3 accumulation within OPTN(E50K) organoids (Figures 7G–7I). As such, disruptions to the autophagy pathway likely contribute to the degeneration of OPTN(E50K) RGCs, with rescue of this phenotype by rapamycin suggesting modulation of autophagy may rescue degenerative phenotypes.

To determine if autophagy disruption was correlated with a decrease in RGC viability, retinal organoids were similarly examined for apoptosis, with OPTN(E50K) organoids exhibiting significantly increased levels of activated caspase-3 found largely within inner layers of these organoids (Figures 7M–7P). In addition, OPTN(E50K) organoids contained significantly fewer BRN3-expressing RGCs, while the number of photoreceptors quantified by expression of OTX2 revealed no significant differences (Figure S3). Retinal organoids were then treated with rapamycin to determine if an association existed between apoptosis and autophagy. When treated with rapamycin, OPTN(E50K) organoids displayed decreased levels of active caspase-3 (Figures 7Q–7S), suggesting an important link between autophagy dysfunction and apoptosis.

Figure 3. OPTN(E50K) RGCs Demonstrate Neurite Deficits at Later Stages of Maturation

(A–P) Inverted fluorescent images (A–H) and representative neurite tracings (I–P) of isogenic control and OPTN(E50K) RGCs from 1 to 4 weeks after purification from retinal organoids. Similar neurite complexity was initially observed, but significant neurite retraction in OPTN(E50K) RGCs became apparent at 4 weeks.

(Q) A significantly lower number of ordered neurites and branch points were observed in OPTN(E50K) RGCs after 4 weeks.

(R and S) OPTN(E50K) RGCs also demonstrated significantly shorter neurites (R) and smaller soma sizes (S) by 4 weeks of maturation. Error bars represent SEM (n = 4 separate differentiation experiments each using OPTN(E50K) hiPSCs, OPTN-corrected hiPSCs, and H7 and H7(E50K) hPSCs) (*$p < 0.05$, **$p < 0.01$, ***$p < 0.001$, ****$p < 0.0001$). Scale bars, 25 μm (A–H) and 100 μm (I–P).

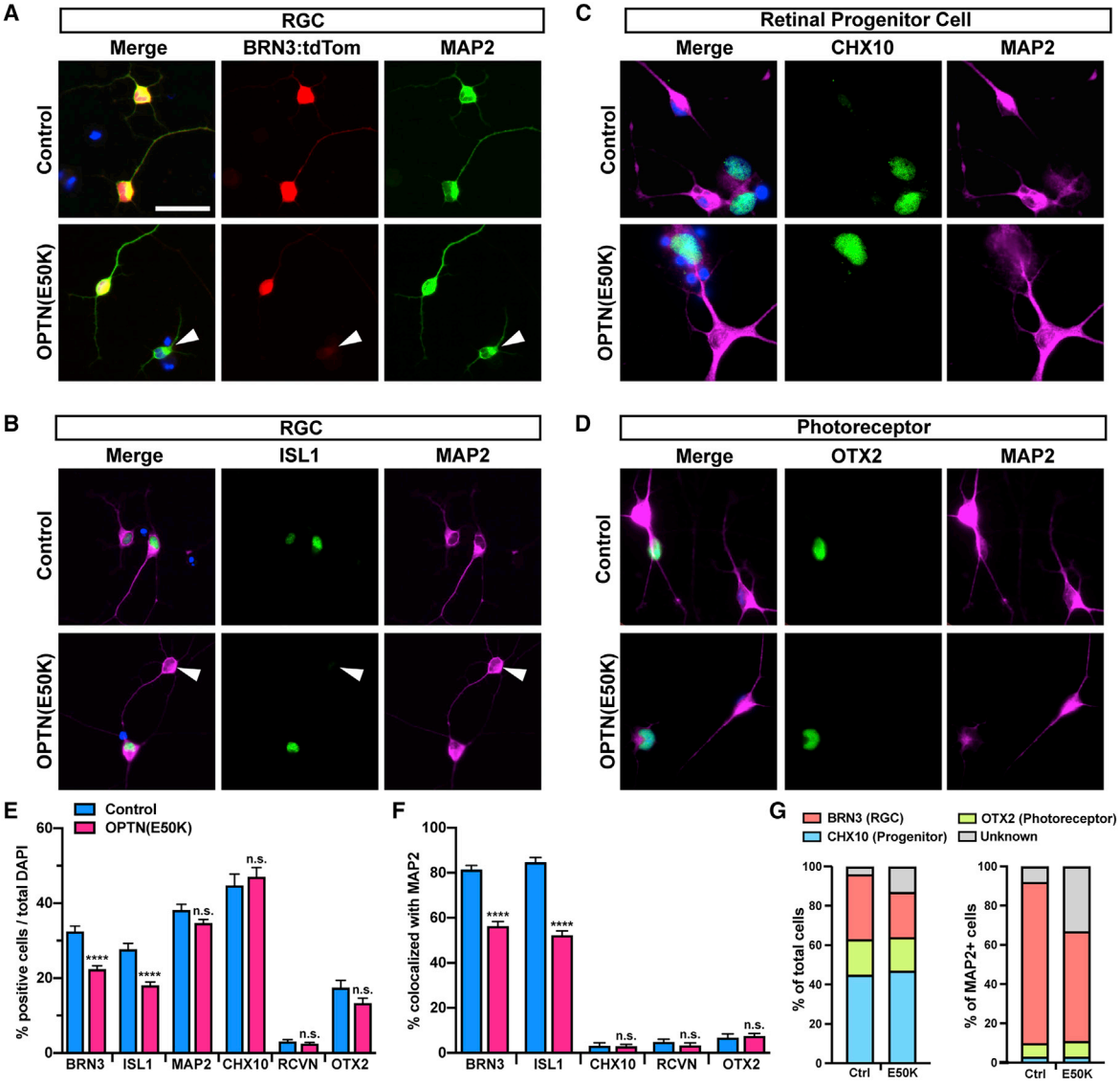

Figure 4. OPTN(E50K) RGCs Downregulate RGC-Associated Transcription Factors

(A and B) The expression of RGC-associated transcription factors BRN3B:tdTomato (A) and ISL1 (B) was correlated with the RGC-associated cytoskeletal marker MAP2, with this correlation decreased in the OPTN(E50K) cell lines.

(C and D) Conversely, minimal correlation was observed between MAP2 and markers of retinal progenitor cells (C, CHX10) and photoreceptors (D, OTX2).

(E) A significant decrease was observed in the expression of BRN3B and ISL1 in OPTN(E50K) RGCs relative to the total number of DAPI-positive cells, with no differences observed in MAP2-expressing cells nor CHX10-expressing retinal progenitor cells or Recoverin/OTX2-expressing photoreceptors.

(F) A significant decrease in co-expression for BRN3 or ISL1 RGCs was observed, with no changes observed for other cell types.

(G) Lastly, as either a percentage of the total cell population or among the MAP2-expressing cells, changes in cell numbers were only observed among RGCs as identified by BRN3 expression. Error bars represent SEM (n = 3 separate differentiation experiments each using OPTN(E50K) hiPSCs, OPTN-corrected hiPSCs, and H7 and H7(E50K) hPSCs) (**$p < 0.01$, ***$p < 0.001$). Scale bars, 25 μm (A–D).

DISCUSSION

hPSCs have been used as a reliable model system for studying both the development of many retinal cell types (Lamba et al., 2006; Lu and Barnstable, 2019; Meyer et al., 2011; Sridhar et al., 2020; Zhong et al., 2014) as well as diseases which result in the degeneration of these cells (Ohlemacher et al., 2016; Sridhar et al., 2018; Teotia

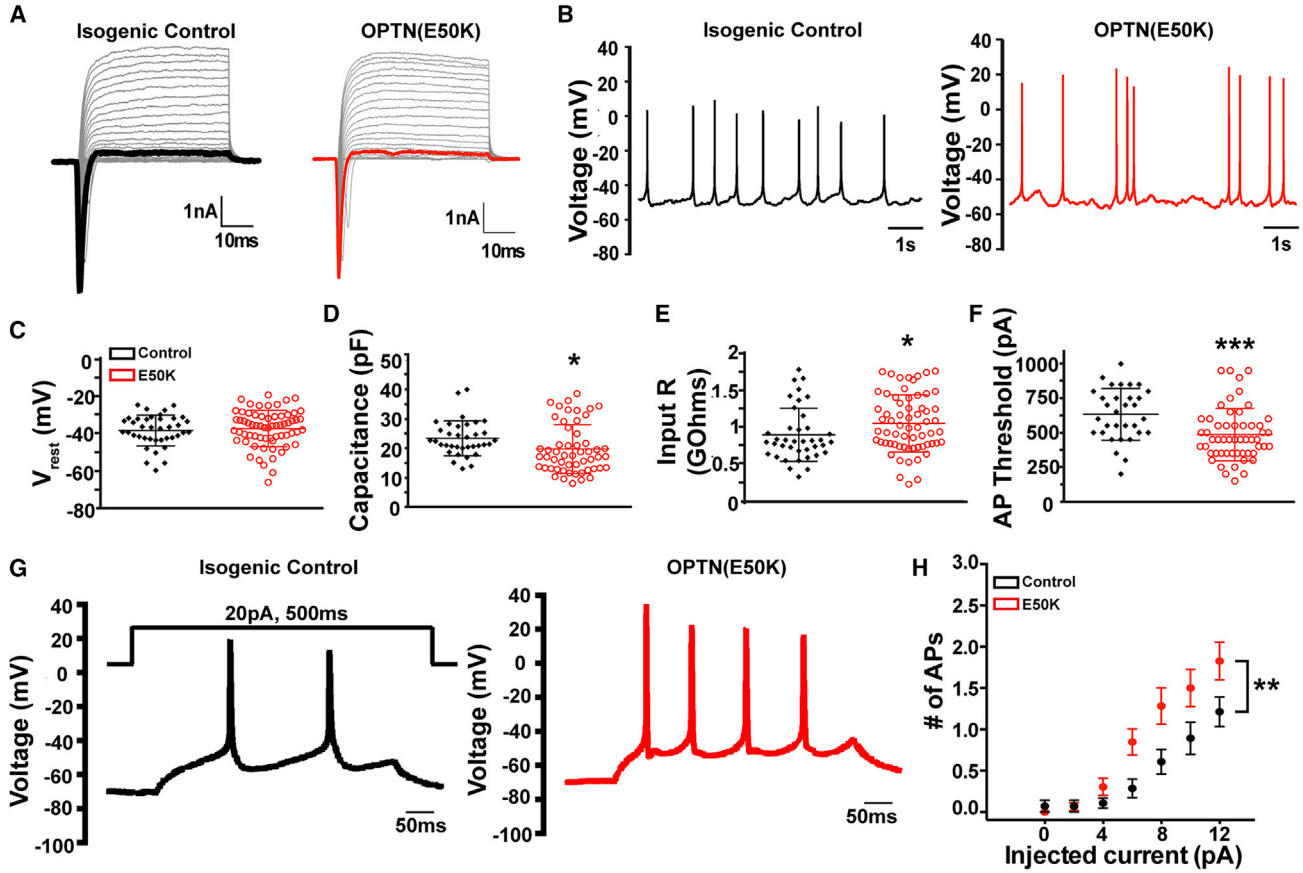

Figure 5. OPTN(E50K) RGCs Display Increased Excitability

(A and B) OPTN(E50K) RGCs and isogenic controls displayed similar abilities to conduct inward sodium and outward potassium currents (A) as well as the ability to fire spontaneous action potentials (B).

(C) No significant differences were identified in the resting membrane potential between OPTN(E50K) RGCs and isogenic controls.

(D–F) OPTN(E50K) RGCs demonstrated significantly lower cell capacitance (D), higher input resistance (E), and a lower action potential current threshold (F) compared with isogenic controls.

(G and H) Representative traces of evoked action potentials (G) following current injections revealed the firing of significantly more action potentials (H) in OPTN(E50K) RGCs compared with isogenic controls. Error bars represent SEM (n = 2 separate differentiation experiments using H7, n = 28 technical replicates and H7(E50K) hPSCs, n = 46 technical replicates) (*p < 0.05, **p < 0.01, ***p < 0.001).

et al., 2017b). The current understanding of glaucomatous neurodegeneration has been established in part by the use of animal models mimicking RGC degeneration and injury (Agostinone et al., 2018; Kalesnykas et al., 2012; Tseng et al., 2015; Williams et al., 2013). Although these studies have been instrumental in discovering various disease phenotypes, important differences exist between rodent and primate retinas (Peng et al., 2019). As such, the use of hPSCs provides a powerful and complimentary model to study RGC development and disease that helps to bridge the gap between rodent studies and human glaucoma patients. Results of the current study demonstrate the most in depth phenotypic and functional characterization of RGCs grown from OPTN(E50K) hPSCs, revealing numerous neurodegenerative phenotypes including autophagy deficits and neurite retraction, allowing for a greater understanding of mechanisms leading to the degeneration and death of RGCs in glaucoma.

CRISPR/Cas9 gene editing provides exciting opportunities for the precise engineering of cells to generate new experimental models (Cong et al., 2013; Muffat et al., 2016; Poon et al., 2017). Of particular interest for this study, CRISPR/Cas9 gene editing allowed for the insertion of disease-causing mutations in hPSCs as well as the correction of these mutations in patient-specific hPSCs, minimizing effects due to variability between cell lines. As previous studies have demonstrated variability in the capacity of numerous hPSC lines to differentiate into retinal cells (Capowski et al., 2019; Meyer et al., 2011),

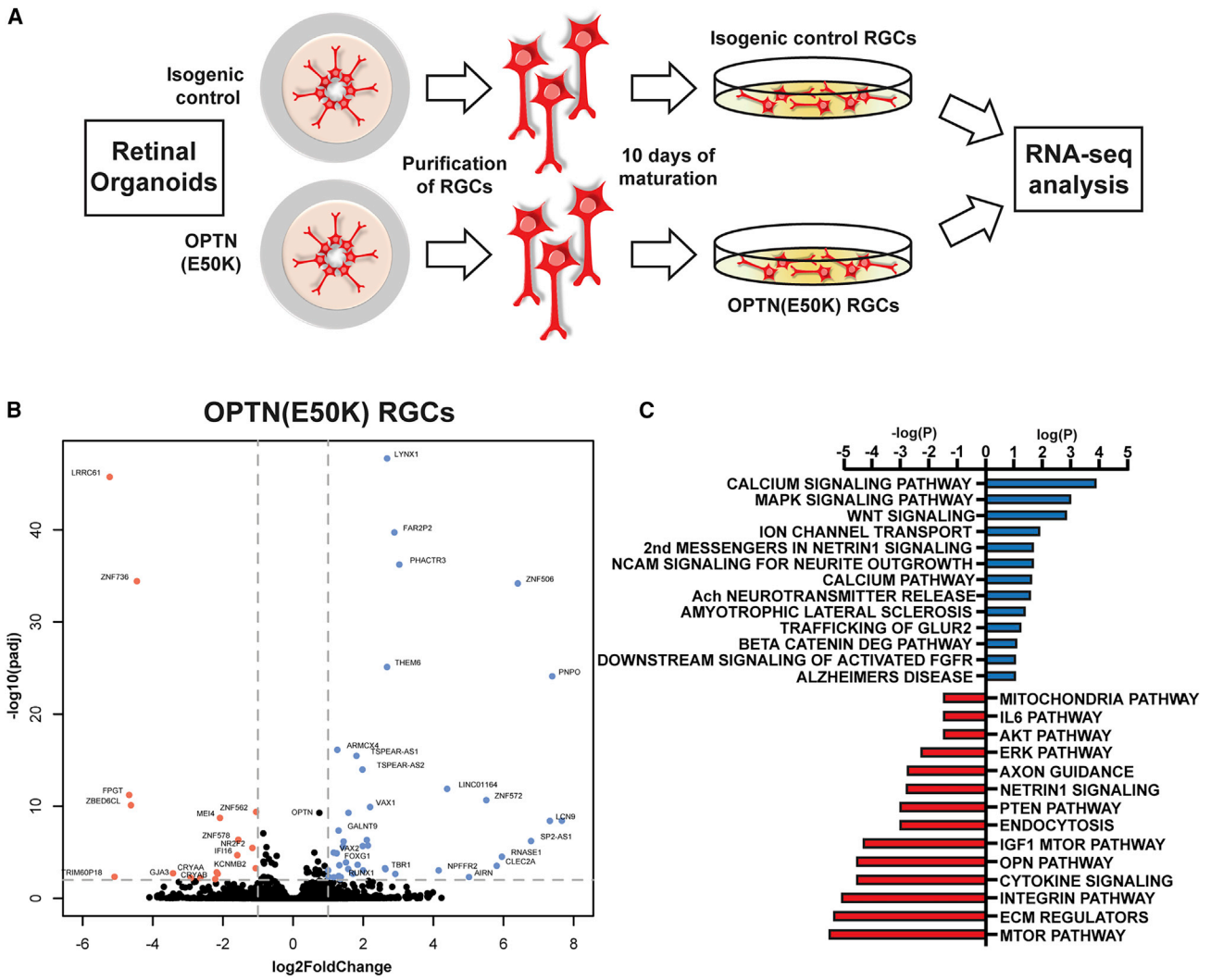

Figure 6. RNA Sequencing Revealed Differential Gene Expression and Pathway Analysis in OPTN(E50K) RGCs

(A) A schematic demonstrates the workflow of RNA sequencing from OPTN(E50K) and isogenic control retinal organoids (n = 4 for isogenic control and n = 4 for OPTN(E50K)).

(B) Differential gene expression analysis demonstrated 75 downregulated genes and 117 upregulated genes in OPTN(E50K) RGCs when compared with isogenic control RGCs ($p < 0.05$).

(C) Pathway analysis revealed a variety of upregulated and downregulated pathways associated with glaucomatous neurodegeneration ($p < 0.1$). n = 5 separate differentiation experiments using H7 and H7(E50K) hPSCs.

this variability complicates the definitive identification of disease-related phenotypes apart from inherent differences between cell lines. The use of CRISPR/Cas9 gene editing in the current study allowed for the definitive identification of disease-related phenotypes directly linked to the OPTN(E50K) mutation. As such, the results of this study provide the foundation for utilizing CRISPR/Cas9 gene editing of hPSCs for the study of other genetically inherited forms of glaucoma as well as other neurodegenerative diseases of the retina to discover mechanisms of degeneration.

The age-related loss of RGCs in glaucoma is characteristic of the loss of neurons found in many neurodegenerative diseases (Chu, 2019; Edens et al., 2016; Gupta and Yucel, 2007; Hartwick, 2001; Hirt et al., 2018; Lai et al., 2017; Mancino et al., 2018; Moloudizargari et al., 2017; Nixon, 2013; Wostyn et al., 2019). In this context, RGCs differentiate normally during early retinogenesis, with degeneration associated with age and disease progression. As such, it is crucial for model systems of glaucoma to demonstrate this type of disease progression *in vitro*. Results of the current study suggested that OPTN(E50K) and isogenic control

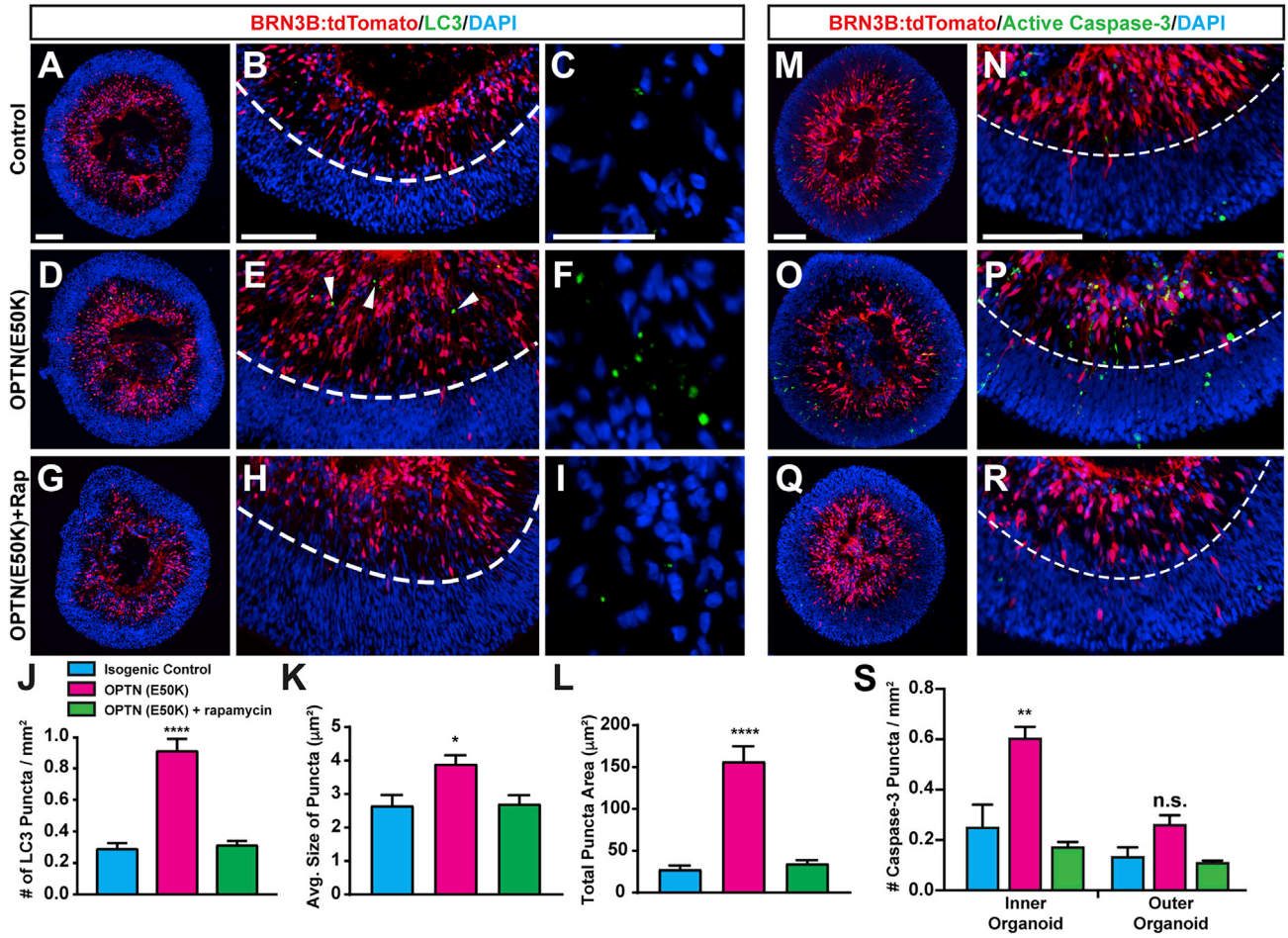

Figure 7. OPTN(E50K) Retinal Organoids Demonstrate Autophagy Dysfunction through LC3 Accumulation

(A–I) Retinal organoids from isogenic control, OPTN(E50K), and OPTN(E50K) plus rapamycin conditions displayed proper organization with BRN3B:tdTomato expression confined within inner layers. Compared with isogenic controls (A–C), LC3 accumulations were found specifically within the inner layers of OPTN(E50K) organoids (D–F), with accumulation rescued by rapamycin treatment (G–I). Arrowheads in (E) indicate LC3 accumulations.

(J–L) Significantly more LC3 puncta (J) were observed in OPTN(E50K) organoids compared with isogenic controls or rapamycin-treated organoids, with accumulations larger in both puncta size (K) and total area (L).

(M–S) OPTN(E50K) retinal organoids (O and P) also displayed significantly higher levels of active caspase-3 within inner layers compared with outer layers as well as corresponding isogenic controls (M and N), with increased active caspase-3 rescued by rapamycin (Q and R). Error bars represent SEM (n = 3 separate differentiation experiments each using OPTN(E50K) hiPSCs, OPTN-corrected hiPSCs, and H7 and H7(E50K) hPSCs) (*$p < 0.05$, ****$p < 0.0001$). Images in (C), (F), and (I) are higher magnification representations of samples analyzed in (B), (E), and (H). Scale bars, 50 μm.

hPSCs both differentiated into early optic cup-like retinal organoids that displayed a lamination of retinal layers. When organoids were dissociated and resultant cells grown in two-dimensional cultures, no significant differences were observed in the initial expression of RGC-associated markers as well as the morphological features of neuronal maturation. Disease phenotypes including neurite retraction, autophagy dysfunction, and apoptosis were only identified in OPTN(E50K) cells after prolonged culture, with this progression somewhat recapitulating the age-related phenotypes observed in glaucomatous neurodegeneration.

The downregulation of RGC-associated transcription factors has been previously established in experimental glaucoma as well as RGC injury models, which provides an early indicator of degeneration in the retina (Soto et al., 2008; Weishaupt et al., 2005). Results of the current study demonstrated the downregulation of the RGC-associated transcription factors BRN3 and ISL1 in OPTN(E50K) RGCs compared with isogenic controls. Importantly, this

downregulation of BRN3 and ISL1 was only identified after prolonged culture, with quantification at earlier time points indicating no significant differences between OPTN(E50K) RGCs and isogenic controls. In future experiments using fluorescent reporters to identify RGCs in hPSC disease models, it will be necessary to account for the downregulation of these reporters to identify those RGCs at advanced stages of the disease state.

The OPTN protein performs a variety of functions within the cell, including its role as an autophagy receptor (Minegishi et al., 2016; Sirohi and Swarup, 2016; Slowicka et al., 2016; Ying et al., 2015; Ying and Yue, 2016). As such, OPTN interacts with a variety of essential autophagy proteins, with the E50K mutation in this protein leading to a disruption in this pathway. Autophagy pathway disruption has also been linked to neurodegeneration in a number of other diseases, including ALS, Alzheimer, and Parkinson diseases, with the possibility of deficits in this pathway conserved as a mechanism leading to the degeneration of neurons (Chu, 2019; Edens et al., 2016; Hirt et al., 2018; Lai et al., 2017; Mancino et al., 2018; Moloudizargari et al., 2017; Nixon, 2013; Wostyn et al., 2019). In this study, results demonstrated profound accumulation of LC3 and significantly higher levels of apoptosis within inner layers compared with both the outer layers of these same organoids as well as the presumptive RGC layers of isogenic controls. When treated with rapamycin, an activator of the autophagy pathway, these phenotypes were reduced back to levels comparable with isogenic controls, reflecting an important balance between the autophagy and apoptotic pathways linked to the OPTN(E50K) mutation.

The overstimulation of cells through excitotoxic mechanisms has been implicated in a variety of neurodegenerative diseases including glaucoma (Cueva Vargas et al., 2015; Dzialo et al., 2013; Hynd et al., 2004). Results of this study demonstrated that OPTN(E50K) RGCs exhibited a significantly lower action potential current threshold than isogenic controls, leading to the firing of significantly more action potentials, with these results suggesting that the increased excitability of OPTN(E50K) RGCs may serve as a key contributor to their degeneration. Importantly, both OPTN(E50K) and isogenic control RGCs were identified for patch-clamp recordings based upon their expression of BRN3B:tdTomato fluorescence. Given that the results of this study also documented the downregulation of BRN3B:tdTomato in more advanced stages of OPTN(E50K) RGC maturation, the possibility exists that the phenotypes observed may represent an earlier stage of the degenerative process, with these phenotypes more severe in those RGCs which are more advanced in their degeneration and have downregulated the tdTomato reporter.

Although glaucoma is often overlooked as a neurodegenerative disease, it bears many similarities to other CNS diseases, such as Parkinson, ALS, and Alzheimer, which ultimately result in the degeneration of neurons in either the brain or spinal cord (Chu, 2019; Edens et al., 2016; Gupta and Yucel, 2007; Hirt et al., 2018; Lai et al., 2017; Mancino et al., 2018; Moloudizargari et al., 2017; Nixon, 2013; Wostyn et al., 2019). Similar to previous studies of RGC damage as well as cortical neurons in Alzheimer disease (Agostinone and Di Polo, 2015; Agostinone et al., 2018; Kalesnykas et al., 2012; Williams et al., 2013), results of this study identified numerous deficits including the downregulation of important RGC transcription factors, neurite retraction, autophagy disruption, and apoptosis, as well as heightened excitability of RGCs, all of which have previously been associated with other neurodegenerative diseases. As such, the results and assays conducted in this study are not only relevant to the study of glaucoma, but also to many other diseases of the CNS, with the possibility to work collectively on targeted therapeutics at these distinctive pathways.

Overall, the results of this study demonstrate a detailed characterization of the OPTN(E50K) mutation and how it affects the degeneration of RGCs. More so, this study extensively utilized CRISPR/Cas9 gene-editing technology for the generation of disease models as well as isogenic controls for studies of glaucoma, with an important emphasis on the discrimination between mutation-causing phenotypes and cell line variability. In future studies using hPSC-based models of glaucomatous neurodegeneration, the identification of other unique neurodegenerative phenotypes and specific pathways leading to those phenotypes should be considered to better target therapeutic strategies.

EXPERIMENTAL PROCEDURES

CRISPR/Cas9 Gene Editing

The OPTN(E50K) mutation was inserted into H7BRN3B:tdTomato-Thy1.2-hESCs (Sluch et al., 2017; Thomson et al., 1998) and an hiPSC line harboring the OPTN(E50K) mutation (Ohlemacher et al., 2016) was corrected (see Supplemental Experimental Procedures for details). Electroporation was performed using the Neon transfection system and, subsequently, cells were plated onto Matrigel-coated plates in mTeSR1 medium with CloneR supplement (STEMCELL Technologies). Forty-eight hours after electroporation, GFP-positive cells were isolated by FACS to enrich for edited cells. After initial growth, clonal populations were isolated and expanded. To screen for the insertion/correction, genomic DNA from individual clones was extracted, and the portion of the OPTN gene containing the 50th codon was amplified by PCR. This PCR product was then enzymatically digested by Hpy188III and run on a 1% gel. Properly edited clones were further confirmed by Sanger sequencing, and chromosomal abnormalities were analyzed by G-banded karyotyping.

Maintenance of hPSCs

hPSCs were cultured from OPTN(E50K) disease lines and corresponding isogenic controls based on previously described protocols (Fligor et al., 2020; Meyer et al., 2011; Ohlemacher et al., 2015). In brief, hPSC colonies were maintained on a Matrigel-coated six-well plate in mTeSR1 medium, with daily medium changes. hPSCs were passaged every 4–5 days based upon their confluency. Before passaging, hPSCs were marked for areas of spontaneous differentiation and those areas were mechanically removed. At 70% confluency, hPSCs were enzymatically passaged with dispase (2 mg/mL) for approximately 15 min and split at a ratio of 1:6 onto a new six-well plate freshly coated with Matrigel.

Differentiation of RGCs

hPSCs were differentiated into retinal organoids and RGCs using an established protocol with minor modifications (Fligor et al., 2020; Ohlemacher et al., 2015). In brief, enzymatically passaged hPSC colonies were grown in suspension to produce embryoid bodies (EBs). Within the first 3 days of differentiation, EBs were slowly transitioned from mTesR1 medium into neural induction medium. On day 6 of differentiation, BMP4 (50 ng/mL) was added to the flask (Capowski et al., 2019). The same medium was used at day 8 to induce adherence of EBs to a plate supplemented with 10% fetal bovine serum. Half of the medium was changed at day 9 and 12 to slowly reduce the concentration of BMP4. At day 15, early optic vesicle colonies were mechanically lifted and transferred into retinal differentiation medium, with a medium change every 2 to 3 days. At 30 days of differentiation, early retinal organoid cultures were supplemented with GlutaMAX and 2% fetal bovine serum to aid in retinal organization. By day 45, retinal organoids were either enzymatically dissociated in Accutase for RGC purification, or preserved as floating organoids for cryosectioning. For some experiments, retinal organoids were treated with rapamycin (2 μM) for 24 h and then fixed for immunocytochemistry.

To purify RGCs, retinal organoids were enzymatically dissociated into single cells using Accutase for 20 min at 37°C. Single-cell suspensions were then enriched for RGCs with the Thy1.2 surface receptor using the MACS cell separation kit (Sluch et al., 2017). A total of 10,000 RGCs were plated on poly-D-ornithine and laminin-coated 12-mm coverslips and maintained for up to 4 weeks in BrainPhys medium (Bardy et al., 2015; VanderWall et al., 2019). To analyze neurite complexity, RGCs were transfected with GFP using lipofectamine 2 days before fixation to aid in identification of individual RGC neurites along with BRN3:tdTomato expression.

Immunocytochemistry

Samples were fixed with 4% paraformaldehyde in phosphate-buffered solution (PBS) for 30 min followed by 3 PBS washes. Retinal organoids were then prepared for cryosectioning through an incubation in 20% sucrose solution for 1 h at room temperature, followed by an incubation in 30% sucrose solution overnight at 4°C. The following day, retinal organoids were transferred into OCT cryostat molds and snap-frozen on dry ice. Sections (12 μm) were cut and used for immunocytochemical analyses.

Following fixation or sectioning, samples were permeabilized in 0.2% Triton X-100 for 10 min at room temperature. Samples were then washed with PBS and blocked with 10% donkey serum for 1 h at room temperature. Primary antibodies (Table S1) were diluted in 0.1% Triton X-100 and 5% donkey serum and applied overnight at 4°C. The next day, the primary antibody was removed and samples were washed three times with PBS and blocked with 10% donkey serum for 10 min at room temperature. Secondary antibodies were diluted at 1:1,000 ratio in 0.1% Triton X-100 and 5% donkey serum and applied to samples for 1 h at room temperature. The secondary antibodies were then removed and samples were washed three times with PBS before mounting onto slides for imaging. Immunofluorescent images were obtained using a Leica DM5500 fluorescence microscope.

Data Quantification

Isogenic control and OPTN(E50K) RGCs were collected at 1, 2, 3, and 4 weeks after purification and analyzed based on neurite complexity, neurite length, and soma size. Several immunofluorescent images were taken of RGCs co-expressing tdTomato and GFP, and soma area and neurite complexity were quantified using ImageJ and Photoshop, with the NeuronJ plugin used to quantify the length of RGC neurites.

Organoids from isogenic control, OPTN(E50K), and OPTN(E50K) plus rapamycin sources were collected at 2.5 months of differentiation and quantified for expression of BRN3, OTX2, and caspase-3 using the cell counter plugin in ImageJ. LC3 puncta number, size, and area were quantified using the ImageJ particle analyzer. Organoid areas were also quantified using ImageJ plugins. For caspase-3 quantification, organoid sections were imaged and the inner and outer layers were traced based on the expression of BRN3:tdTomato in Photoshop. The areas of inner and outer layers were determined using ImageJ and the cell counter plugin was used to quantify caspase-3 fragments in each layer.

Statistical Analyses

Statistical significance for neurite complexity, soma size, neurite length, and electrophysiological recordings was performed using two-tailed Student's t test and significance based on a p value of < 0.05. Significance for BRN3 and ISL1 quantifications were achieved by a Student's t test based on a p value of < 0.05. For BRN3, OTX2, caspase-3, and LC3 accumulations, a one-way ANOVA followed by a Tukey's post hoc analysis was used to determine significance based on a p value < 0.05.

Electrophysiology

Whole-cell patch-clamp recordings were performed at room temperature (~22°C) using a HEKA EPC-10 amplifier as described previously (VanderWall et al., 2019), with detail provided in Supplemental Experimental Procedures. RGCs were identified by tdTomato fluorescence. To enhance comparisons between cells during action potential activity recording, current was injected to bias the cell membrane potential to −70 mV. Current threshold for action potential generation was obtained by a series of 1-ms stimuli of increasing intensity, with the maximum number of action potentials elicited measured during a series of 500-ms stimuli of increasing intensity. Voltage-clamp recordings were obtained from each cell at the end of the series of current-clamp protocols. The peak amplitudes of sodium and potassium currents were

measured using a standard I-V protocol with a holding potential at −80 mV. The current density was calculated by normalizing current amplitude to the capacitance of each cell.

RNA Sequencing Preparation and Analysis

RGCs were immunopurified from organoids after 45 days of differentiation and grown in adherent cultures for 10 days in BrainPhys medium. RNA was collected using the PicoPure RNA isolation kit. Total RNA was evaluated for its quantity and quality using an Agilent Bioanalyzer 2100. Approximately 30 million reads per library were generated. The sequencing data were next assessed using FastQC (Babraham Bioinfomatics, Cambridge, UK) and then mapped to the human genome (GRCH38) using STAR RNA sequencing aligner (Dobin et al., 2013). Differentially expressed genes were tested by using DESeq2 with a false discovery rate < 0.05 as the significant cutoff (Love et al., 2014). Pathway enrichment analysis were conducted by hypergeometric test against human gene ontology and MsigDB v.6 canonical pathways, with $p < 0.01$ as the significant cutoff (Subramanian et al., 2005). The RNA sequencing experiments reported in this paper have been deposited in the Gene Expression Omnibus database, www.ncbi.nih.gov/geo (accession no. GSE145069).

DATA AND CODE AVAILABILITY

All sequencing data have been deposited to GEO under accession number GEO: GSE145069.

SUPPLEMENTAL INFORMATION

Supplemental Information can be found online at https://doi.org/10.1016/j.stemcr.2020.05.009.

AUTHOR CONTRIBUTIONS

K.B.V. and K.-C.H. designed the experiments, collected and analyzed the data, and wrote the manuscript. Y.P., S.S.L., P.T., and C.Z. collected and analyzed the data. C.M.F., A.R.A., and K.A.L. collected the data. H.C.T. designed the experiments. T.R.C. designed the experiments and analyzed the data. J.S.M. designed the experiments, analyzed the data, and wrote and approved the manuscript.

ACKNOWLEDGMENTS

We thank Dr. Amelia Linnemann for helpful discussions about autophagy analyses and the sharing of antibodies. We also thank Dr. Don Zack and Dr. Valentin Sluch for sharing the BRN3B:tdTomato:Thy1.2 vectors used in the generation of RGC reporter cell lines. Grant support was provided by the National Eye Institute (R01 EY024984 and R21 EY031120 to J.S.M.), the Indiana Department of Health Spinal Cord and Brain Injury Research Fund (grant no. 26343 to J.S.M.), and an Indiana CTSI Core Pilot grant (to J.S.M.). This publication was also made possible with partial support from a University Fellowship (to K.C.-H.) and from an Indiana CTSI pre-doctoral research fellowship (UL1TR002529, A. Shekhar, PI) from the NIH, National Center for Advancing Translational Sciences, Clinical and Translational Sciences Award (to K.B.V.).

Received: October 24, 2019
Revised: May 12, 2020
Accepted: May 13, 2020
Published: June 11, 2020

REFERENCES

Agostinone, J., Alarcon-Martinez, L., Gamlin, C., Yu, W.Q., Wong, R.O.L., and Di Polo, A. (2018). Insulin signalling promotes dendrite and synapse regeneration and restores circuit function after axonal injury. Brain *141*, 1963–1980.

Agostinone, J., and Di Polo, A. (2015). Retinal ganglion cell dendrite pathology and synapse loss: implications for glaucoma. Prog. Brain Res. *220*, 199–216.

Bardy, C., van den Hurk, M., Eames, T., Marchand, C., Hernandez, R.V., Kellogg, M., Gorris, M., Galet, B., Palomares, V., Brown, J., et al. (2015). Neuronal medium that supports basic synaptic functions and activity of human neurons in vitro. Proc. Natl. Acad. Sci. U S A *112*, E2725–E2734.

Capowski, E.E., Samimi, K., Mayerl, S.J., Phillips, M.J., Pinilla, I., Howden, S.E., Saha, J., Jansen, A.D., Edwards, K.L., Jager, L.D., et al. (2019). Reproducibility and staging of 3D human retinal organoids across multiple pluripotent stem cell lines. Development *146*, dev171686.

Chalasani, M.L., Kumari, A., Radha, V., and Swarup, G. (2014). E50K-OPTN-induced retinal cell death involves the Rab GTPase-activating protein, TBC1D17 mediated block in autophagy. PLoS One *9*, e95758.

Chu, C.T. (2019). Mechanisms of selective autophagy and mitophagy: implications for neurodegenerative diseases. Neurobiol. Dis. *122*, 23–34.

Cong, L., Ran, F.A., Cox, D., Lin, S., Barretto, R., Habib, N., Hsu, P.D., Wu, X., Jiang, W., Marraffini, L.A., et al. (2013). Multiplex genome engineering using CRISPR/Cas systems. Science *339*, 819–823.

Cueva Vargas, J.L., Osswald, I.K., Unsain, N., Aurousseau, M.R., Barker, P.A., Bowie, D., and Di Polo, A. (2015). Soluble tumor necrosis factor alpha promotes retinal ganglion cell death in glaucoma via calcium-permeable AMPA receptor activation. J. Neurosci. *35*, 12088–12102.

Dobin, A., Davis, C.A., Schlesinger, F., Drenkow, J., Zaleski, C., Jha, S., Batut, P., Chaisson, M., and Gingeras, T.R. (2013). STAR: ultrafast universal RNA-seq aligner. Bioinformatics *29*, 15–21.

Dzialo, J., Tokarz-Deptula, B., and Deptula, W. (2013). Excitotoxicity and Wallerian degeneration as a process related to cell death in nervous system. Arch. Ital. Biol. *151*, 67–75.

Edens, B.M., Miller, N., and Ma, Y.C. (2016). Impaired autophagy and defective mitochondrial function: converging paths on the road to motor neuron degeneration. Front. Cell. Neurosci. *10*, 44.

Fingert, J.H. (2011). Primary open-angle glaucoma genes. Eye *25*, 587–595.

Fligor, C.M., Huang, K.C., Lavekar, S.S., VanderWall, K.B., and Meyer, J.S. (2020). Differentiation of retinal organoids from human pluripotent stem cells. Methods Cell Biol. https://doi.org/10.1016/bs.mcb.2020.02.005.

Fligor, C.M., Langer, K.B., Sridhar, A., Ren, Y., Shields, P.K., Edler, M.C., Ohlemacher, S.K., Sluch, V.M., Zack, D.J., Zhang, C., et al. (2018). Three-dimensional retinal organoids facilitate the investigation of retinal ganglion cell development, organization and neurite outgrowth from human pluripotent stem cells. Sci. Rep. *8*, 14520.

Gupta, N., and Yucel, Y.H. (2007). Glaucoma as a neurodegenerative disease. Curr. Opin. Ophthalmol. *18*, 110–114.

Hartwick, A.T. (2001). Beyond intraocular pressure: neuroprotective strategies for future glaucoma therapy. Optom. Vis. Sci. *78*, 85–94.

Hirt, J., Porter, K., Dixon, A., McKinnon, S., and Liton, P.B. (2018). Contribution of autophagy to ocular hypertension and neurodegeneration in the DBA/2J spontaneous glaucoma mouse model. Cell Death Discov. *4*, 14.

Hynd, M.R., Scott, H.L., and Dodd, P.R. (2004). Glutamate-mediated excitotoxicity and neurodegeneration in Alzheimer's disease. Neurochem. Int. *45*, 583–595.

Inagaki, S., Kawase, K., Funato, M., Seki, J., Kawase, C., Ohuchi, K., Kameyama, T., Ando, S., Sato, A., Morozumi, W., et al. (2018). Effect of timolol on optineurin aggregation in transformed induced pluripotent stem cells derived from patient with familial glaucoma. Invest. Ophthalmol. Vis. Sci. *59*, 2293–2304.

Kalesnykas, G., Oglesby, E.N., Zack, D.J., Cone, F.E., Steinhart, M.R., Tian, J., Pease, M.E., and Quigley, H.A. (2012). Retinal ganglion cell morphology after optic nerve crush and experimental glaucoma. Invest. Ophthalmol. Vis. Sci. *53*, 3847–3857.

Lai, S.W., Lin, C.L., and Liao, K.F. (2017). Glaucoma may be a non-memory manifestation of Alzheimer's disease in older people. Int. Psychogeriatr. https://doi.org/10.1017/S1041610217000801.

Lamba, D.A., Karl, M.O., Ware, C.B., and Reh, T.A. (2006). Efficient generation of retinal progenitor cells from human embryonic stem cells. Proc. Natl. Acad. Sci. U S A *103*, 12769–12774.

Langer, K.B., Ohlemacher, S.K., Phillips, M.J., Fligor, C.M., Jiang, P., Gamm, D.M., and Meyer, J.S. (2018). Retinal ganglion cell diversity and subtype specification from human pluripotent stem cells. Stem Cell Reports *10*, 1282–1293.

Love, M.I., Huber, W., and Anders, S. (2014). Moderated estimation of fold change and dispersion for RNA-seq data with DESeq2. Genome Biol. *15*, 550.

Lu, A.Q., and Barnstable, C.J. (2019). Pluripotent stem cells as models of retina development. Mol. Neurobiol. *56*, 6056–6070.

Mancino, R., Martucci, A., Cesareo, M., Giannini, C., Corasaniti, M.T., Bagetta, G., and Nucci, C. (2018). Glaucoma and Alzheimer disease: one age-related neurodegenerative disease of the brain. Curr. Neuropharmacol. *16*, 971–977.

Meng, Q., Lv, J., Ge, H., Zhang, L., Xue, F., Zhu, Y., and Liu, P. (2012). Overexpressed mutant optineurin(E50K) induces retinal ganglion cells apoptosis via the mitochondrial pathway. Mol. Biol. Rep. *39*, 5867–5873.

Meyer, J.S., Howden, S.E., Wallace, K.A., Verhoeven, A.D., Wright, L.S., Capowski, E.E., Pinilla, I., Martin, J.M., Tian, S., Stewart, R., et al. (2011). Optic vesicle-like structures derived from human pluripotent stem cells facilitate a customized approach to retinal disease treatment. Stem Cells *29*, 1206–1218.

Minegishi, Y., Iejima, D., Kobayashi, H., Chi, Z.L., Kawase, K., Yamamoto, T., Seki, T., Yuasa, S., Fukuda, K., and Iwata, T. (2013). Enhanced optineurin E50K-TBK1 interaction evokes protein insolubility and initiates familial primary open-angle glaucoma. Hum. Mol. Genet. *22*, 3559–3567.

Minegishi, Y., Nakayama, M., Iejima, D., Kawase, K., and Iwata, T. (2016). Significance of optineurin mutations in glaucoma and other diseases. Prog. Retin. Eye Res. *55*, 149–181.

Moloudizargari, M., Asghari, M.H., Ghobadi, E., Fallah, M., Rasouli, S., and Abdollahi, M. (2017). Autophagy, its mechanisms and regulation: implications in neurodegenerative diseases. Ageing Res. Rev. *40*, 64–74.

Muffat, J., Li, Y., and Jaenisch, R. (2016). CNS disease models with human pluripotent stem cells in the CRISPR age. Curr. Opin. Cell Biol. *43*, 96–103.

Nixon, R.A. (2013). The role of autophagy in neurodegenerative disease. Nat. Med. *19*, 983–997.

Ohlemacher, S.K., Iglesias, C.L., Sridhar, A., Gamm, D.M., and Meyer, J.S. (2015). Generation of highly enriched populations of optic vesicle-like retinal cells from human pluripotent stem cells. Curr. Protoc. Stem Cell Biol. *32*, 1h.8.1–1h.8.20.

Ohlemacher, S.K., Sridhar, A., Xiao, Y., Hochstetler, A.E., Sarfarazi, M., Cummins, T.R., and Meyer, J.S. (2016). Stepwise differentiation of retinal ganglion cells from human pluripotent stem cells enables analysis of glaucomatous neurodegeneration. Stem Cells *34*, 1553–1562.

Peng, Y.R., Shekhar, K., Yan, W., Herrmann, D., Sappington, A., Bryman, G.S., van Zyl, T., Do, M.T.H., Regev, A., and Sanes, J.R. (2019). Molecular classification and comparative taxonomics of foveal and peripheral cells in primate retina. Cell *176*, 1222–1237.e2.

Poon, A., Zhang, Y., Chandrasekaran, A., Phanthong, P., Schmid, B., Nielsen, T.T., and Freude, K.K. (2017). Modeling neurodegenerative diseases with patient-derived induced pluripotent cells: possibilities and challenges. New Biotechnol. *39*, 190–198.

Quigley, H.A. (2011). Glaucoma. Lancet *377*, 1367–1377.

Rezaie, T., Child, A., Hitchings, R., Brice, G., Miller, L., Coca-Prados, M., Heon, E., Krupin, T., Ritch, R., Kreutzer, D., et al. (2002). Adult-onset primary open-angle glaucoma caused by mutations in optineurin. Science *295*, 1077–1079.

Sarfarazi, M., Stoilov, I., and Schenkman, J.B. (2003). Genetics and biochemistry of primary congenital glaucoma. Ophthalmol. Clin. North Am. *16*, 543–554, vi.

Sirohi, K., and Swarup, G. (2016). Defects in autophagy caused by glaucoma-associated mutations in optineurin. Exp. Eye Res. *144*, 54–63.

Slowicka, K., Vereecke, L., and van Loo, G. (2016). Cellular functions of optineurin in health and disease. Trends Immunol. *37*, 621–633.

Sluch, V.M., Chamling, X., Liu, M.M., Berlinicke, C.A., Cheng, J., Mitchell, K.L., Welsbie, D.S., and Zack, D.J. (2017). Enhanced stem cell differentiation and immunopurification of genome engineered human retinal ganglion cells. Stem Cell Transl. Med. *6*, 1972–1986.

Soto, I., Oglesby, E., Buckingham, B.P., Son, J.L., Roberson, E.D., Steele, M.R., Inman, D.M., Vetter, M.L., Horner, P.J., and Marsh-Armstrong, N. (2008). Retinal ganglion cells downregulate gene expression and lose their axons within the optic nerve head in a mouse glaucoma model. J. Neurosci. *28*, 548–561.

Sridhar, A., Hoshino, A., Finkbeiner, C.R., Chitsazan, A., Dai, L., Haugan, A.K., Eschenbacher, K.M., Jackson, D.L., Trapnell, C., Bermingham-McDonogh, O., et al. (2020). Single-cell transcriptomic comparison of human fetal retina, hPSC-derived retinal organoids, and long-term retinal cultures. Cell Rep. *30*, 1644–1659.e4.

Sridhar, A., Langer, K.B., Fligor, C.M., Steinhart, M., Miller, C.A., Ho-A-Lim, K.T., Ohlemacher, S.K., and Meyer, J.S. (2018). Human pluripotent stem cells as in vitro models for retinal development and disease. In Regenerative Medicine and Stem Cell Therapty for the Eye, B.G. Ballios and M.J. Young, eds. (Springer), pp. 17–49.

Subramanian, A., Tamayo, P., Mootha, V.K., Mukherjee, S., Ebert, B.L., Gillette, M.A., Paulovich, A., Pomeroy, S.L., Golub, T.R., Lander, E.S., et al. (2005). Gene set enrichment analysis: a knowledge-based approach for interpreting genome-wide expression profiles. Proc. Natl. Acad. Sci. U S A *102*, 15545–15550.

Tanaka, T., Yokoi, T., Tamalu, F., Watanabe, S., Nishina, S., and Azuma, N. (2015). Generation of retinal ganglion cells with functional axons from human induced pluripotent stem cells. Sci. Rep. *5*, 8344.

Teotia, P., Chopra, D.A., Dravid, S.M., Van Hook, M.J., Qiu, F., Morrison, J., Rizzino, A., and Ahmad, I. (2017a). Generation of functional human retinal ganglion cells with target specificity from pluripotent stem cells by chemically defined recapitulation of developmental mechanism. Stem Cells *35*, 572–585.

Teotia, P., Van Hook, M.J., Wichman, C.S., Allingham, R.R., Hauser, M.A., and Ahmad, I. (2017b). Modeling glaucoma: retinal ganglion cells generated from induced pluripotent stem cells of patients with SIX6 risk allele show developmental abnormalities. Stem Cells *35*, 2239–2252.

Thomson, J.A., Itskovitz-Eldor, J., Shapiro, S.S., Waknitz, M.A., Swiergiel, J.J., Marshall, V.S., and Jones, J.M. (1998). Embryonic stem cell lines derived from human blastocysts. Science *282*, 1145–1147.

Tseng, H.C., Riday, T.T., McKee, C., Braine, C.E., Bomze, H., Barak, I., Marean-Reardon, C., John, S.W., Philpot, B.D., and Ehlers, M.D. (2015). Visual impairment in an optineurin mouse model of primary open-angle glaucoma. Neurobiol. Aging *36*, 2201–2212.

VanderWall, K.B., Vij, R., Ohlemacher, S.K., Sridhar, A., Fligor, C.M., Feder, E.M., Edler, M.C., Baucum, A.J., 2nd, Cummins, T.R., and Meyer, J.S. (2019). Astrocytes regulate the development and maturation of retinal ganglion cells derived from human pluripotent stem cells. Stem Cell Reports *12*, 201–212.

Weishaupt, J.H., Klocker, N., and Bahr, M. (2005). Axotomy-induced early down-regulation of POU-IV class transcription factors Brn-3a and Brn-3b in retinal ganglion cells. J. Mol. Neurosci. *26*, 17–25.

Williams, P.A., Howell, G.R., Barbay, J.M., Braine, C.E., Sousa, G.L., John, S.W., and Morgan, J.E. (2013). Retinal ganglion cell dendritic atrophy in DBA/2J glaucoma. PLoS One *8*, e72282.

Wostyn, P., Van Dam, D., and De Deyn, P.P. (2019). Alzheimer's disease and glaucoma: look-alike neurodegenerative diseases. Alzheimers Dement. *15*, 600–601.

Ying, H., Turturro, S., Nguyen, T., Shen, X., Zelkha, R., Johnson, E.C., Morrison, J.C., and Yue, B.Y. (2015). Induction of autophagy in rats upon overexpression of wild-type and mutant optineurin gene. BMC Cell Biol. *16*, 14.

Ying, H., and Yue, B.Y. (2016). Optineurin: the autophagy connection. Exp. Eye Res. *144*, 73–80.

Zhong, X., Gutierrez, C., Xue, T., Hampton, C., Vergara, M.N., Cao, L.H., Peters, A., Park, T.S., Zambidis, E.T., Meyer, J.S., et al. (2014). Generation of three-dimensional retinal tissue with functional photoreceptors from human iPSCs. Nat. Commun. *5*, 4047.